Stability of Foam Films and Surface Rheology: An Oscillating Bubble Study at Low Frequencies

Cosima Stubenrauch*,† and Reinhard Miller‡

Institut für Physikalische Chemie, Universität zu Köln, Luxemburger Strasse 116, D-50939 Köln, Germany, and Max-Planck-Institut für Kolloid- und Grenzflächenforschung, Am Mühlenberg 1, D-14476 Golm, Germany

Received: January 21, 2004; In Final Form: March 1, 2004

The dilational surface elasticity ϵ and the dilational surface viscosity η of the two nonionic surfactants *n*-dodecyl-β-D-maltoside (β-$C_{12}G_2$) and tetraethyleneglycol-monodecyl ether ($C_{10}E_4$) were studied using the oscillating drop method. The experiments were carried out at different concentrations and frequencies with an accessible frequency range of 0.005−0.2 Hz. The results are discussed in the light of previous disjoining pressure measurements that demonstrated that the stability of thin liquid films cannot be explained solely by the magnitude of the surface forces. Indeed, a comparison of the results obtained for β-$C_{12}G_2$ with those obtained for $C_{10}E_4$ reveals a correlation between the stability of the films and the surface dilational elasticity of the respective monolayers.

1. Introduction

"Equal surface forces do not automatically result in equal foam film stabilities." This observation has been found experimentally for both ionic[1] and nonionic surfactants.[2−4] An example is given in Figure 1, where the disjoining pressure Π is presented as a function of the film thickness h for aqueous solutions of the two nonionic surfactants *n*-dodecyl-β-D-maltoside (β-$C_{12}G_2$) and tetraethyleneglycol-monodecyl ether ($C_{10}E_4$).

The disjoining pressure Π is a measure of the repulsive surface forces per unit area acting normal to the surfaces in a thin liquid film.[6] Supposing that the origin of the disjoining pressure is an electrostatic repulsion,[7,8] one can fit the $\Pi(h)$ curves with the DLVO theory, which leads to an effective surface charge. For the sake of clarity, we will focus on the stability of the electrostatically stabilized common black films (CBF) and leave out the Newton black films (NBF), which are stabilized by short-range confinement forces (for details see refs 3−5). In Figure 1a the $\Pi(h)$ curves of a 6.85×10^{-5} M β-$C_{12}G_2$ and of a 1.1×10^{-4} M $C_{10}E_4$ solution are shown. With respect to the surface forces, no significant difference can be detected between the two $\Pi(h)$ curves; in both cases the surface charge density q_0 is calculated to be 1.17 mC m^{-2}. However, the corresponding foam film stabilities are far from being comparable. Whereas the β-$C_{12}G_2$ film is stable up to 9000 Pa, the $C_{10}E_4$ film already ruptures at pressures around 800 Pa. In other words, the β-$C_{12}G_2$ film is much more stable than the corresponding $C_{10}E_4$ film, although both systems have the same surface charge density. Moreover, a look at Figure 1b reveals that the stability of the CBF increases with increasing $C_{10}E_4$ concentration, whereas for β-$C_{12}G_2$ the reverse is observed. It is important to realize that the increase of the film stability in the case of $C_{10}E_4$ is accompanied by a decrease of the surface charge density, which, in turn, destabilizes the film. To sum up, one can conclude that neither the low stability of the $C_{10}E_4$ film at $q_0 = 1.17$ mC m^{-2} (Figure 1a) nor the increasing stability of the $C_{10}E_4$ film with decreasing surface charge (Figure 1b) can be explained in terms of surface forces.

As the stability of thin liquid films obviously cannot be explained solely by the magnitude of the repulsion forces operating normal to the film surfaces, the ability of the monolayers to absorb energy tangentially to the surface comes into play. What we need is a surface that is able to dampen external disturbances, thus preventing the film from rupturing. This ability is believed to be mirrored in the surface viscoelasticity of the monolayer. In connection with this, a correlation between the limiting (high-frequency) dilational elasticity and the film stability is often claimed. However, discussing the stability of foam films in terms of Gibbs elasticities not only can be misleading but can also lead to unphysical results. For example, the limiting elasticities of the solutions with which the $\Pi(h)$ curves shown in Figure 1a were measured are 138 mN m^{-1} for the β-$C_{12}G_2$ and 200 mN m^{-1} for the $C_{10}E_4$ solution, respectively. However, the films of the former solution are much more stable than those of the latter. Note that the stability we are referring to in this context is not the lifetime of the film but a measure for the maximum pressure that can be applied to the film.

Considering that the limiting elasticity is excluded, it is obviously the frequency-dependent dilational (or compression) surface elasticity and the dilational surface viscosity that are the appropriate parameters to quantify and/or characterize the stability of foam films.[1,9−12] As the monolayer is directly connected with the bulk phase, the dilational parameters depend strongly on adsorption and desorption processes. Compressing (expanding) the monolayer leads to desorption (adsorption) of the surfactant molecules into (from) the bulk to restore the equilibrium surface concentration. Two extreme cases are easy to understand: when the frequency of a sinusoidal perturbation is low, the monolayer has time to reach equilibrium, and there is no resistance to the deformations. When the frequency is high, the monolayer has no time to respond and behaves as if it were insoluble. The situation is even more complex because the time to reach equilibrium strongly depends on the surfactant concentration. Thus, the surface rheological parameters are a

* Corresponding author. E-mail: stubenrauch@uni-koeln.de.
† Universität zu Köln.
‡ Max-Planck-Institut für Kolloid- und Grenzflächenforschung.

10.1021/jp049694e CCC: $27.50
Published on Web 04/23/2004

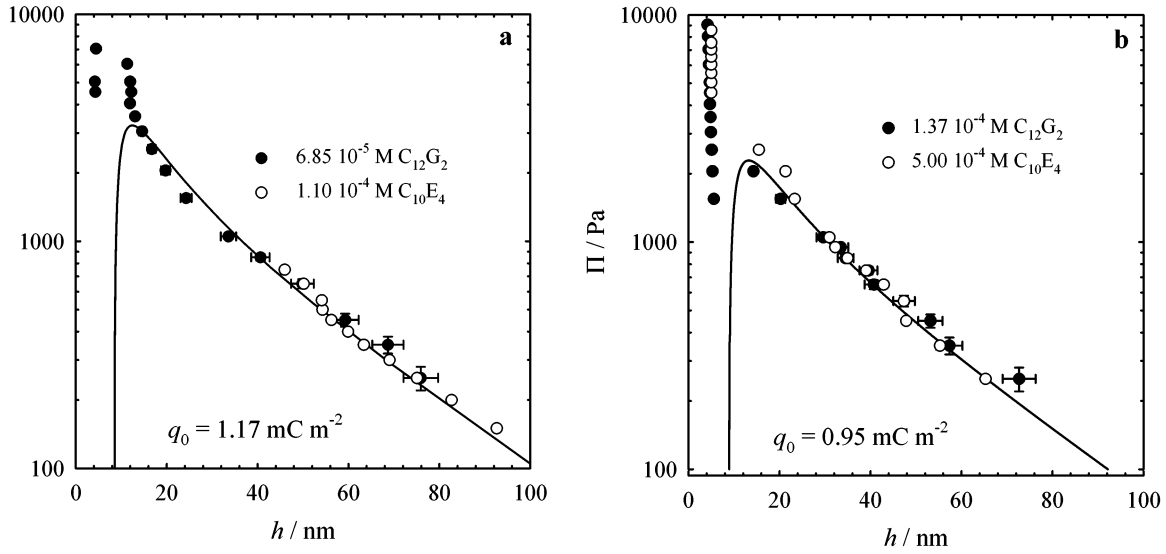

Figure 1. $\Pi(h)$ curves of thin liquid foam films stabilized by aqueous solutions of β-$C_{12}G_2$ and $C_{10}E_4$. All concentrations are below the cmc (cmc($C_{10}E_4$) = 8.6×10^{-4} M, cmc(β-$C_{12}G_2$) = 1.7×10^{-4} M). The solutions contain 10^{-4} M NaCl. The data are fitted with the DLVO theory from which the surface charge density is calculated to be $q_0 = 1.17$ mC m^{-2} (Figure 1a) and $q_0 = 0.95$ mC m^{-2} (Figure 1b), respectively. Data are taken from refs 3−5.

function of both the frequency and the concentration, the interrelations of which are complicated.

The aim of the oscillating bubble study at hand was to investigate the correlation between the stability of foam films and surface rheological parameters for the two particular surfactants mentioned above, namely, β-$C_{12}G_2$ and $C_{10}E_4$. For that purpose, we measured dilational surface elasticities (ϵ) and viscosities (η) as a function of the surfactant concentration and the frequency. The investigated frequency range was 0.005−0.20 Hz, and the concentrations investigated were equal to those for which the respective $\Pi(h)$ curves have already been measured. The influence of the frequency and the surfactant concentration on the elasticities and viscosities is shown, and the results are discussed in view of the corresponding $\Pi(h)$ curves. Furthermore, the data obtained for β-$C_{12}G_2$ and $C_{10}E_4$ will be compared with literature data and related to the ongoing discussion on which parameters are suitable to describe the stability of thin liquid foam films.

2. Experimental Section

2.1. Materials and Cleaning Procedure. The nonionic surfactants *n*-dodecyl-β-D-maltoside (β-$C_{12}G_2$) and tetraethyleneglycol-monodecyl ether ($C_{10}E_4$) were purchased from Sigma (Germany) and Bachem (Germany), respectively. The solutions were prepared with Milli-Q water. Sodium chloride (NaCl) was obtained from Merck (Germany) and roasted at 500 °C overnight to remove organic contaminants. All glassware was cleaned either with deconex from Borer Chemie (as a replacement for chromic sulfuric acid) or with concentrated sulfuric acid and rinsed thoroughly with water before use. Note that the rheological measurements have been carried out with the same solutions investigated in the disjoining pressure studies.[3−5] Thus all surfactant solutions contain 10^{-4} M NaCl, although neither the surface tension nor the rheological parameters are sensitive to these low electrolyte concentrations. To check the purity of the surfactants, the surface tensions were measured at 22 °C by the Du Noüy ring method, using a Krüss K10ST tensiometer. The surface tension isotherms of β-$C_{12}G_2$ and $C_{10}E_4$ (see Figure 2) do not indicate any contaminations, so that the surfactants were used as received.

The $\sigma(\log c)$ were fitted with the Langmuir−Szyszkowski equation

$$\sigma = \sigma_0 - RT\Gamma_\infty \ln\left(1 + \frac{c}{a}\right) \quad (1)$$

where $\sigma_0 = 72.2$ mN m^{-1} is the surface tension of the solvent, Γ_∞ is the maximum surface concentration of surfactant, and a represents the concentration at which 50% of Γ_∞ has been reached. The best fitting parameters for (a) β-$C_{12}G_2$ are $\Gamma_\infty = 4.45 \times 10^{-6}$ mol m^{-2} and $a = 4.59 \times 10^{-6}$ M,[13] and (b) $C_{10}E_4$ are $\Gamma_\infty = 3.32 \times 10^{-6}$ mol m^{-2} and $a = 4.48 \times 10^{-6}$ M.[5] The Langmuir adsorption model is not an optimum description for the studied surfactants but suitable for the present purpose. A more detailed analysis of the adsorption behavior will be published elsewhere.

2.2. Surface Rheological Measurements. The surface rheological measurements were carried out with the profile analysis tensiometer PAT1 from SINTERFACE.[14] The main principle of this method is to determine the surface tension σ of a liquid from the shape of a pendent drop by fitting the Gauss−Laplace equation to the coordinates of the drop.[15] The drop is formed at the tip of a capillary, and a computer-controlled dosing system generates oscillations of the drop volume. To guarantee that an equilibrated surface oscillates, the surface tension is measured as a function of time until the equilibrium value is reached. For the investigated solutions a duration of 3000 s was sufficient to reach equilibrium, which is demonstrated by the corresponding σ values shown in Figure 2. The equilibrated surface is then disturbed by sinusoidal oscillations (the accessible frequency range is 0.001−0.2 Hz), which cause sinusoidal changes in the surface area and the radius, i.e., in the drop shape. The changes in drop shape are monitored by a video camera, and the corresponding changes in surface tension are calculated. In addition, one obtains information about the phase shift between the sinusoidal disturbance and the sinusoidal response of the system. From these data the dilational surface elasticity and viscosity are calculated via a Fourier transformation algorithm as described in ref 14. Two exemplary experiments are shown in Figure 3.

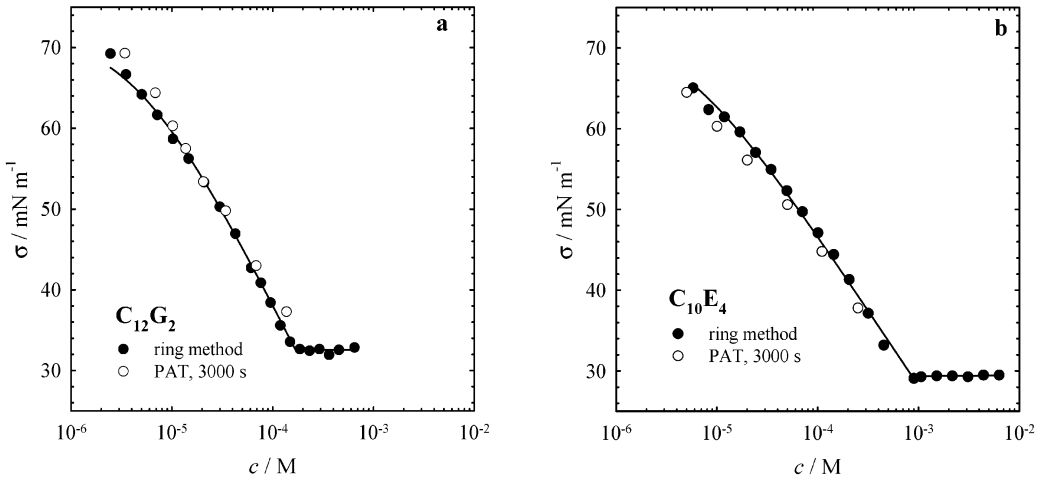

Figure 2. Surface tension isotherms of the two investigated surfactants β-$C_{12}G_2$ (a) and $C_{10}E_4$ (b). The curves show no minimum or flattening around the cmc, which demonstrates the purity of the surfactants. The error is about the size of the symbols. The lines represent the best Langmuir−Szyszkowski fits, leading to cmc values of 1.7×10^{-4} M for β-$C_{12}G_2$ and 8.6×10^{-4} M for $C_{10}E_4$, respectively. The data obtained by the ring method are taken from ref 13 for β-$C_{12}G_2$ and from ref 5 for $C_{10}E_4$. To demonstrate the reliability and accuracy of the PAT measurements, the surface tensions of all investigated surfactant solutions measured after 3000 s are also shown (open symbols).

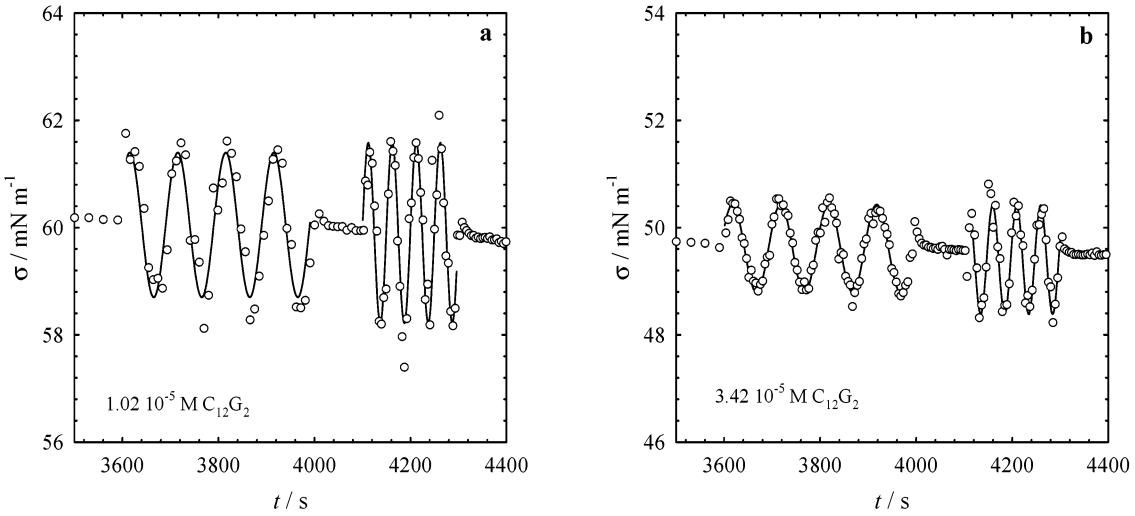

Figure 3. Experimentally determined surface tensions of an oscillating drop. Results are shown (a) for a 1.02×10^{-5} M and (b) for a 3.42×10^{-5} M β-$C_{12}G_2$ solution. The frequencies with which the drops oscillate are 0.01 and 0.02 Hz, respectively. The solid lines are calculated according to eq 2 with the parameters given in Table 1.

TABLE 1: Results of the Fourier Transformation Algorithm with Which the Dilational Surface Elasticity ϵ and Viscosity η Are Calculated[14] [a]

c/M	ν/Hz	A/mN m^{-1}	σ_{mean}/mN m^{-1}	ϕ/deg	ϵ/mN m^{-1}	η/s mN m^{-1}
1.02×10^{-5}	0.01	1.37 ± 0.02	60.1 ± 0.1	24.8 ± 1.0	18.0 ± 0.5	121 ± 4
	0.02	1.68 ± 0.01	59.9 ± 0.1	20.8 ± 1.0	22.0 ± 0.5	62 ± 3
3.42×10^{-5}	0.01	0.82	49.6	31.7	10.5	88
	0.02	1.02	49.4	32.2	13.0	56

[a] Data are given for two different concentrations c of β-$C_{12}G_2$. ν is the frequency with which the drop oscillates, A the amplitude of the surface tension oscillations, σ_{mean} the mean surface tension, and ϕ the phase shift between sinusoidal disturbance and response. The error of the calculated parameters does not exceed 5%.

The lines are calculated according to

$$\sigma(t) = \sigma_{mean} + A \sin(2\pi t\nu + \phi) \qquad (2)$$

where σ_{mean} is the mean interfacial tension, A the amplitude of the surface tension oscillations, ν the frequency with which the drop oscillates, and ϕ the phase shift between sinusoidal disturbance and response. The parameters calculated by the algorithm for the two experiments shown in Figure 3 are given in Table 1.

3. Results and Discussion

3.1. Theoretical Background and Data Evaluation. The dilational surface elasticity ϵ and viscosity η are the real part and the imaginary part, respectively, of the complex modulus $\bar{\epsilon}$, which describes the linear response of a surfactant monolayer to a sinusoidal deformation of frequency ν, i.e.,

$$\bar{\epsilon} = \epsilon + i\omega\eta \qquad (3)$$

It was already outlined in the Introduction that the surface

elasticity ϵ and the surface viscosity η are a function of both the frequency ν and the surfactant bulk concentration c. Equations for $\epsilon(\nu,c)$ and $\eta(\nu,c)$ were first derived by van den Tempel and Lucassen.[16] According to their model, there are no adsorption/desorption barriers at the interface, and exchanges between bulk and surface are controlled by simple diffusion. With these assumptions one obtains

$$\epsilon(\nu,c) = \epsilon_0 \frac{1+\xi}{1+2\xi+2\xi^2} \tag{4}$$

and

$$\eta(\nu,c) = \frac{\epsilon_0}{2\pi\nu} \frac{\xi}{1+2\xi+2\xi^2} \tag{5}$$

with

$$\xi = \sqrt{\frac{\omega_0}{4\pi\nu}}$$

Thus, the parameters ϵ_0 and ω_0 determine the $\epsilon(\nu,c)$ and $\eta(\nu,c)$ curves. The former is the high-frequency limit of the elasticity (according to eq 4, one obtains $\epsilon = \epsilon_0$ for $\nu \rightarrow \infty$), which coincides with the limiting elasticity obtained from the respective equation of state

$$\epsilon_0 = -\Gamma \frac{d\sigma}{dc} \frac{dc}{d\Gamma} \tag{6}$$

In the following, ϵ_0 will always be referred to as the theoretical high-frequency limit of the elasticity to avoid confusion. The second parameter is the molecular exchange parameter

$$\omega_0 = D\left(\frac{dc}{d\Gamma}\right)^2 \tag{7}$$

with D being the diffusion coefficient of surfactant molecules in the bulk phase. According to eqs 6 and 7, ϵ_0 and ω_0 are determined by the first and second derivatives of the respective equation of state, i.e., $d\sigma/dc$ and $d^2\sigma/dc^2$, which is proportional to $d\Gamma/dc$. Thus, at first sight, it should be possible to calculate the frequency and concentration dependencies of ϵ and η, respectively, if the equation of state is known. However, a comparison of the experimentally determined high-frequency limit of the elasticity and the respective calculated value of ϵ_0 reveals unacceptably large differences, especially at high concentrations.[9,17−20] Whereas the theoretical ϵ_0 value increases continuously with increasing surfactant concentration, the experimental one reaches a plateau. The reasons for these differences are discussed controversially.[17,18,21−23] We will come back to this point below. What is important for the paper at hand is the fact that the frequency range investigated does not include the high-frequency limit, so that ϵ_0 could not be determined experimentally. Thus, we regard here ϵ_0 and ω_0 as fitting parameters. The fitting procedure was carried out such that couples of $\epsilon_{0,fit}$ and $\omega_{0,fit}$ values were determined that best describe both the experimental $\epsilon(\nu,c)$ and $\eta(\nu,c)$ curves.

3.2. Frequency Dependence of the Surface Viscoelasticity. To investigate the frequency dependence of the surface elasticity ϵ and the surface viscosity η, measurements in a range from 0.005 to 0.20 Hz have been carried out. In Figure 4 data of the sugar surfactant β-$C_{12}G_2$ (a) and of the alkyl polyglycol ether $C_{10}E_4$ (b) for three different surfactant concentrations are presented.

The observation that the elasticity increases whereas the viscosity decreases continuously with increasing frequency is in agreement with eqs 4 and 5, respectively. However, for the concentrations investigated the frequencies are too low to reach the high-frequency limit, i.e., $\epsilon = \epsilon_0$ and $\eta = 0$. It is only at the lowest concentration of 10^{-5} M that a tendency to reach a plateau value for ϵ is visible. In the case of $C_{10}E_4$ this tendency is even accompanied by η values close to zero, so that the highest frequencies investigated are indeed not far from the limiting elasticity for this particular solution. We will come back to this point later on. As was described in section 3.1, we fitted the results according to eqs 4 and 5 with $\epsilon_{0,fit}$ and $\omega_{0,fit}$ being the fitting parameters. As is seen in Figure 4, the experimental data can be described very well with the model of van den Tempel and Lucassen. It is only for the surface viscosities η of the 1.1×10^{-4} M $C_{10}E_4$ solution that significant deviations between the experimental and the calculated data are seen. This is most probably due to the low η values, the experimental determination of which is very difficult.

After determining the fitting parameters $\epsilon_{0,fit}$ and $\omega_{0,fit}$, we calculated the corresponding theoretical values ϵ_0 and ω_0. On the assumption of a Langmuir−Szyszkowski adsorption isotherm (eq 1) eqs 6 and 7 turn into

$$\epsilon_0 = RT\Gamma_\infty \frac{c}{a} \tag{6a}$$

and

$$\omega_0 = D\left(\frac{(a+c)^2}{\Gamma_\infty a}\right)^2 \tag{7a}$$

To calculate ϵ_0 and ω_0 the Langmuir−Szyszkowski parameters given in section 2 and diffusion coefficients of 3.5×10^{-10} m^2 s^{-1} for β-$C_{12}G_2$ and 2.5×10^{-10} m^2 s^{-1} for $C_{10}E_4$, respectively, were used (see section 3.3). The resulting fitting parameters $\epsilon_{0,fit}$ and $\omega_{0,fit}$ as well as ϵ_0 and ω_0 are listed in Table 2. For the sake of comparison literature data of C_{13}DMPO are also provided.[18]

The results presented in Table 2 illustrate two points that are worth mentioning. The first is the fact that the values of $\epsilon_{0,fit}$ and $\omega_{0,fit}$ increase with increasing surfactant concentration. As $\epsilon_{0,fit}$ is the high-frequency limit, an increase in the bulk concentration simply leads to an increase of the surface concentration, which, in turn, increases the elasticity. The increase of $\omega_{0,fit}$ is simply due to the fact that an increase of both the bulk and the surface concentrations leads to a faster molecular exchange. (Note that $\omega_{0,fit}$ does not depend on the frequency ν.) The second point of relevance is the discrepancy between the fitting parameters $\epsilon_{0,fit}$ and $\omega_{0,fit}$ and the theoretical values ϵ_0 and ω_0, which increases with increasing surfactant concentration. A discrepancy between experimental and theoretical values of ϵ_0 and ω_0 is in agreement with previous results and believed to be due to an inaccurate equation of state[9,17,18] or the neglect of the recently introduced two-dimensional compressibility of the surface layer.[21−23] Moreover, it is important to realize that $\epsilon_{0,fit}$ and $\omega_{0,fit}$ might deviate from the experimental high-frequency limits. Thus it is above all the high-frequency range that has to be investigated in order to obtain accurate experimental values for ϵ_0 and ω_0, which then can be compared with the theoretical ones. Work to clarify this point is under way.

Undoubtedly, measurements at higher frequencies are needed to gain a deeper insight into the surface rheological properties

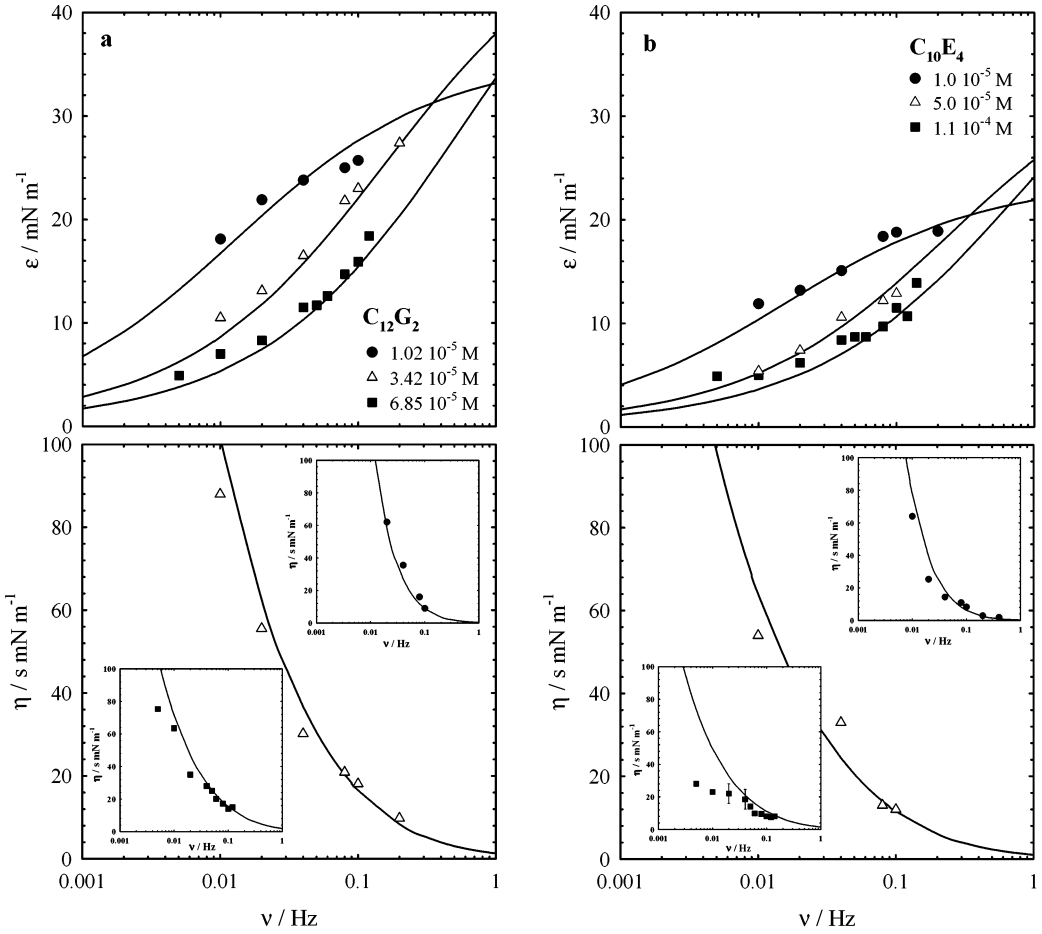

Figure 4. Dilational surface elasticities ϵ and viscosities η of (a) β-$C_{12}G_2$ and (b) $C_{10}E_4$, respectively, as a function of the frequency ν for three different concentrations. All concentrations are below the cmc (cmc(β-$C_{12}G_2$) = 1.7×10^{-4} M, cmc($C_{10}E_4$) = 8.6×10^{-4} M). The solid lines are calculated according to eqs 4 and 5 with the parameters given in Table 2. Insets: For the sake of clarity the surface viscosities are shown separately.

TABLE 2: Surface Rheological Parameters of β-$C_{12}G_2$, $C_{10}E_4$, and C_{13}DMPO[a]

	c/M	ϵ_0/mN m^{-1}	$\epsilon_{0,\mathrm{fit}}$/mN m^{-1}	ω_0/s^{-1}	$\omega_{0,\mathrm{fit}}$/s^{-1}
β-$C_{12}G_2$	1.02×10^{-5}	21	36	0.04	0.08
$\Gamma_\infty = 4.45 \times 10^{-6}$ mol m^{-2}	3.42×10^{-5}	69	51	2.0	1.0
$a = 4.59\ 10^{-6}$ M	6.85×10^{-5}	138	58	23	3.6
$D = 3.5 \times 10^{-10}$ m^2 s^{-1}					
$C_{10}E_4$	1.0×10^{-5}	19	24	0.05	0.1
$\Gamma_\infty = 3.32 \times 10^{-6}$ mol m^{-2}	2.0×10^{-5}	37	24	0.4	0.1[b]
$a = 4.48 \times 10^{-6}$ M	5.0×10^{-5}	92	37	10	1.5
$D = 2.5 \times 10^{-10}$ m^2 s^{-1}	1.1×10^{-4}	200	44	135	4.5
C_{13}DMPO	5.0×10^{-6}	30	33	0.0018	0.0036
$\Gamma_\infty = 4.7 \times 10^{-6}$ mol m^{-2}	1.0×10^{-5}	59	51	0.094	0.30[c]
$a = 1.93 \times 10^{-6}$ M	2.0×10^{-5}	119	53	0.27	1.40
$D = 5 \times 10^{-10}$ m^2 s^{-1}	5.0×10^{-5}	297	53	1.46	44.2

[a] The theoretical values ϵ_0 and ω_0 were calculated according to eqs 6a and 7a. The values of $\epsilon_{0,\mathrm{fit}}$ and $\omega_{0,\mathrm{fit}}$ were obtained by fitting the experimental curves with eqs 4 and 5, respectively. Data of C_{13}DMPO are taken from ref 18. [b] Data are not shown in Figure 4. [c] The value given in ref 18 is a misprint (D. Wantke, personal communication).

and to get more accurate fitting parameters. However, $\epsilon_{0,\mathrm{fit}}$ and $\omega_{0,\mathrm{fit}}$ have the correct order of magnitude and thus can be used to estimate not only the high-frequency limit of the elasticity but also the frequency above which this constant value will be reached, namely, at frequencies $\nu > \omega_{0,\mathrm{fit}}$. We can now understand why it is only at the lowest concentration of 10^{-5} M that a tendency to reach a constant value for ϵ is visible. At this concentration the molecular exchange parameter is on the order of the maximum frequency accessible by our experiment, i.e., $\nu \approx \omega_{0,\mathrm{fit}}$. For all other concentrations we find $\nu \ll \omega_{0,\mathrm{fit}}$, so that the monolayer cannot be considered to be insoluble because the molecular exchange between the bulk and the surface plays the decisive role.

To conclude this section we will present a comparison between our data and those obtained by Wantke et al. for C_{13}-DMPO.[18] Note that these authors determined the amplitude $|\epsilon|$ of the complex modulus $\bar{\epsilon}$, whereas in the present paper the real part ϵ of $\bar{\epsilon}$ has been measured. According to $|\epsilon| = \epsilon/\cos\phi$ (see Appendix, eq A2), we divided our data by cos ϕ in order to compare the results. (Note that it was not possible to determine the real part ϵ from Wantke's data, as they could not determine all ϕ values with the required accuracy.) In Figure 5 the frequency dependence of $|\epsilon|$ is shown for β-$C_{12}G_2$, $C_{10}E_4$, and C_{13}DMPO at a chosen surfactant concentration of 10^{-5} M.

Qualitatively the results agree perfectly well. At low frequencies the amplitude $|\epsilon|$ increases with increasing frequency for

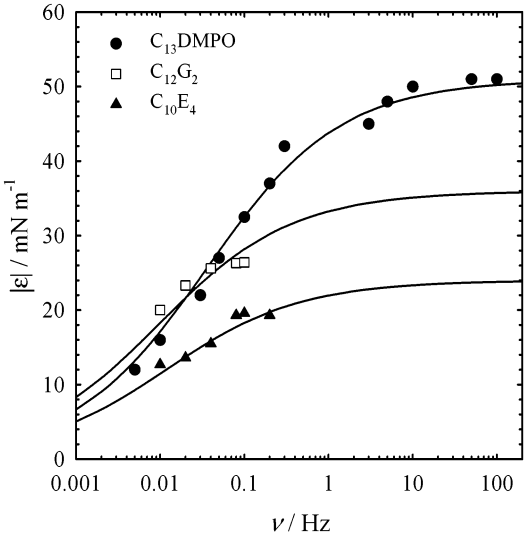

Figure 5. Amplitudes $|\epsilon|$ of the complex elasticity modulus $\bar{\epsilon}$ of C_{13}DMPO, β-$C_{12}G_2$, and $C_{10}E_4$ as a function of the frequency ν at a concentration of 10^{-5} M. This concentration is below the cmc for all three surfactants: cmc (C_{13}DMPO) = 1.0×10^{-4} M [24], cmc(β-$C_{12}G_2$) = 1.7×10^{-4} M, cmc($C_{10}E_4$) = 8.6×10^{-4} M. The data for C_{13}DMPO are taken from ref 18. The solid lines are calculated according to eq A4 (see Appendix) with the parameters given in Table 2.

all three surfactants. Moreover, the data of Wantke et al.[18] confirm the model of van den Tempel and Lucassen over a broad frequency range including the fact that a high-frequency limit is eventually reached. It is important to realize that the elasticity depends on the properties of the monolayer formed at the water−air interface. As equal bulk concentrations do not result in equal surface concentrations, the differences seen in Figure 5 are mainly due to different adsorption layers. In other words, a quantitative comparison is only reasonable at equal surface concentrations and therefore goes beyond the scope of the present paper. Additionally, different methods work at different experimental conditions, so that deviations can have their origin here as well (profile analysis tensiometry in the paper at hand and oscillating bubble method in ref 18). Speculative though it might be, we expect different surface rheological parameters at equal surface concentrations, reflecting different interactions of the surfactant molecules in the monolayer. Note that, at each frequency, the surface elasticity of the 10^{-5} M C_{13}DMPO solution is higher than the elasticities of the respective β-$C_{12}G_2$ and $C_{10}E_4$ solutions. Thus, at this particular concentration, thin liquid films stabilized by C_{13}DMPO are expected to be the most stable. We will come back to this point in section 3.4.

3.3. Concentration Dependence of the Surface Viscoelasticity. We have already discussed that the surface rheological parameters depend not only on the frequency but also on the concentration. Having a closer look at Figure 4, one sees that at low frequencies the elasticity decreases with increasing surfactant concentration, whereas the opposite is observed for the high-frequency limit of the elasticities (see Table 2). This difference can be understood if one investigates the concentration dependence of the surface elasticity at constant frequency. In Figure 6 dilational surface elasticities ϵ and viscosities η of (a) β-$C_{12}G_2$ and (b) $C_{10}E_4$ as a function of the concentration c for three different frequencies are shown. The solid lines are calculated according to eqs 4 and 5. Note that in contrast to the calculations made in section 3.2 the parameters ϵ_0 and ω_0 cannot be used as fitting parameters because they also depend on the concentration. Thus, $\epsilon_0(c)$ and $\omega_0(c)$ were calculated according to eqs 6a and 7a, respectively, with the parameters given in Table 2. The only free parameter was the diffusion coefficient, which was determined to be 3.5×10^{-10} m^2 s^{-1} for β-$C_{12}G_2$ and 2.5×10^{-10} m^2 s^{-1} for $C_{10}E_4$.[25]

It can be seen in Figure 6 that the experimental data $\epsilon(c)$ and $\eta(c)$ run through a maximum at concentrations around 10^{-5} M and that this maximum is slightly shifted toward higher concentrations with increasing frequency. Qualitatively these results agree perfectly well with low-frequency measurements performed with $C_{12}E_6$[26−28] as well as with high-frequency measurements performed with different alkyl trimethylammonium bromides (C_nTAB).[9,10,29] Quantitative differences between our results and those obtained for $C_{12}E_6$ and the C_nTABs are mainly due to the different adsorption properties of the surfactants and to the different frequencies at which the investigations have been carried out. We will come back to this point below. Coming back to Figure 6 the questions to be answered are the following: (a) Why do the curves run through a maximum with increasing concentration? (b) Why is the maximum of the curves shifted toward higher concentrations with increasing frequency? (c) What is the reason for the differences seen between experimental and calculated data? For the sake of clarity we will focus on the $\epsilon(c)$ curves to answer these questions.

Let us first answer the question why the elasticity ϵ runs through a maximum with increasing surfactant concentration. An increase of the surfactant concentration c has two different effects. On one hand, the surface concentration Γ is increased, which, in turn, leads to a higher elasticity ϵ_0 according to eq 6. On the other hand, the molecular exchange between bulk and surface is increased with increasing surfactant concentration c. It is because of this fast exchange that at high concentrations any surface tension gradient $d\sigma$ is evened out immediately, which results in $\epsilon = 0$. Thus, at low concentrations it is the increasing surface concentration Γ, whereas at high concentrations it is the molecular exchange that determines the $\epsilon(c)$ curves. This "crossover" is mirrored in a maximum of the $\epsilon(c)$ curve. It has to be mentioned that the concentration of the maximum is not supposed to be equal for β-$C_{12}G_2$ and $C_{10}E_4$ (see Figure 6). The concentration at which the maximum occurs depends on the molecular exchange parameter ω_0 and thus—according to eq 7—on the static and dynamic adsorption properties of the particular surfactant. For example, measurements carried out with $C_{12}E_6$ at low frequencies[28] resulted in maxima of the $\epsilon(c)$ curves at concentrations around 10^{-6} M. Thus different adsorption parameters are usually expected to lead to different maxima in the respective $\epsilon(c)$ curves. However, owing to the limited number of data points, an exact determination of the concentrations at the maxima was not possible in the study at hand.

Let us address the second observation, namely, that the maximum of the $\epsilon(c)$ curve shifts toward higher concentrations with increasing frequency. When discussing surface elasticities, we always have to take into account two different frequencies, namely, the frequency of disturbance ν and the frequency of the molecular exchange ω_0. We have seen that we simply have to increase the surfactant concentration to obtain a maximum in the $\epsilon(c)$ curve at constant frequency ν. In this way the molecular exchange becomes faster and a "crossover" from $\omega_0 < \nu$ to $\omega_0 > \nu$ takes place. Therefore, the higher the frequency ν, the higher the surfactant concentration c required for the "crossover". This trend is illustrated in Figure 7a, where the amplitude $|\epsilon|$ of C_{13}DMPO is plotted as a function of the concentration for three different frequencies.[30] At 0.1 and 1 Hz the maximum is reached around a concentration of 10^{-5} M (the concentration shift that is expected to occur between 0.1 and 1

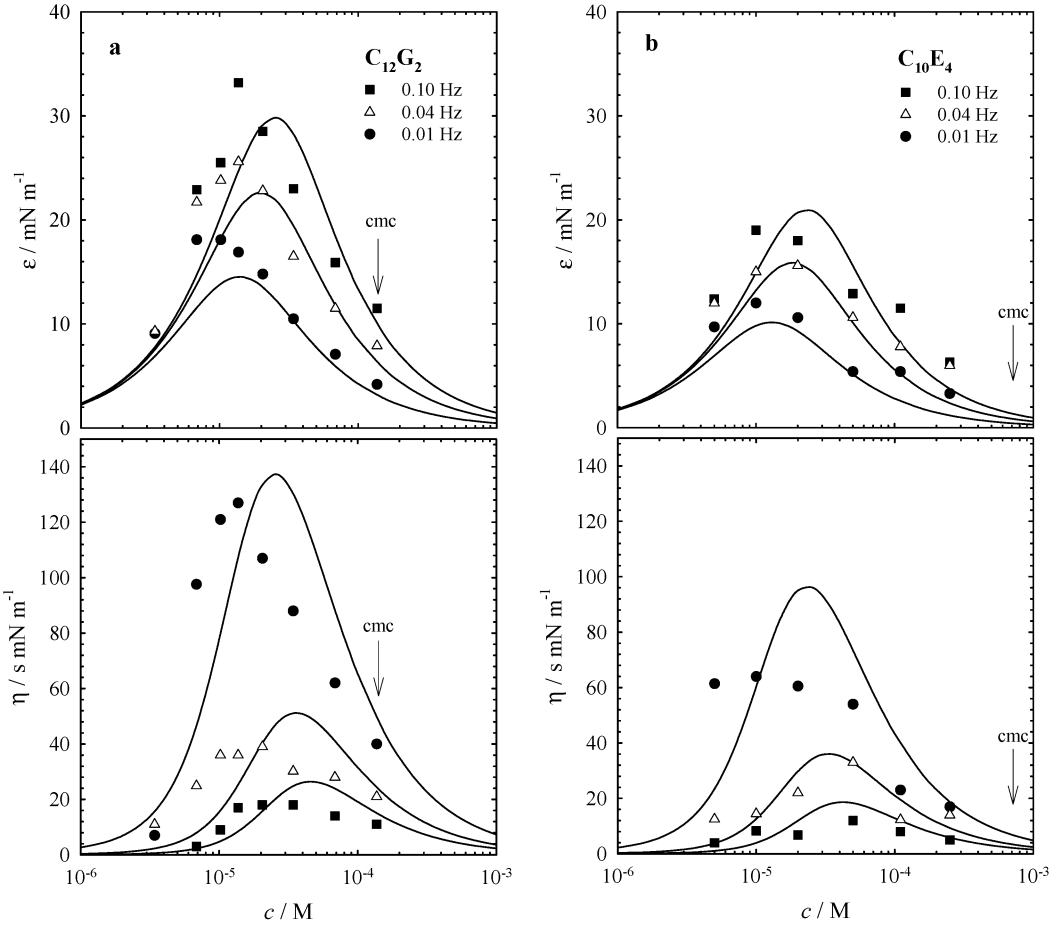

Figure 6. Dilational surface elasticities ϵ and viscosities η of (a) β-$C_{12}G_2$ and (b) $C_{10}E_4$, respectively, as a function of the concentration c for three different frequencies. The cmc is indicated by an arrow (cmc(β-$C_{12}G_2$) = 1.7×10^{-4} M, cmc($C_{10}E_4$) = 8.6×10^{-4} M). The solid lines are calculated according to eqs 4 and 5. The concentration-dependent parameters ϵ_0 and ω_0 are calculated according to eqs 6a and 7a, respectively, with the parameters given in Table 2. The diffusion coefficient in eq 7a was regarded as fitting parameter.

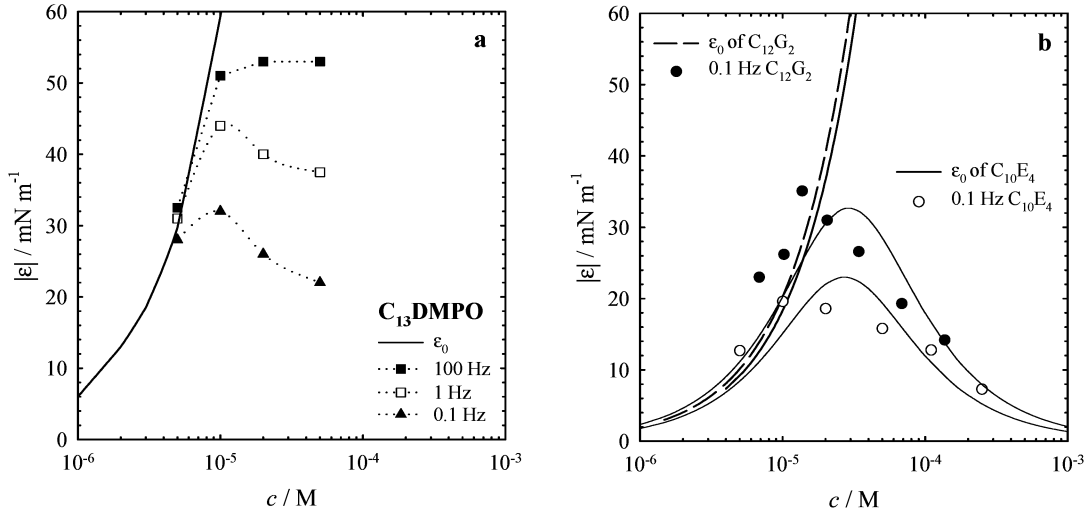

Figure 7. Amplitudes $|\epsilon|$ of the complex modulus $\bar{\epsilon}$ as well as high-frequency limit of the elasticity ϵ_0 of C_{13}DMPO, β-$C_{12}G_2$, and $C_{10}E_4$ as a function of the concentration c. (a) $|\epsilon|$ for C_{13}DMPO at 0.1, 1, and 100 Hz, respectively. Data are taken from ref 18. (b) $|\epsilon|$ for β-$C_{12}G_2$ and $C_{10}E_4$ at 0.1 Hz. The theoretical $|\epsilon|(c)$ curves are calculated according to eq A4 (see Appendix) with the parameters given in Table 2, and the ϵ_0 values are calculated with eq 6a.

Hz cannot be detected due to the small number of available data points), whereas at 100 Hz the $|\epsilon|$ values increase up to 5×10^{-5} M (a decrease is expected at $c > 5 \times 10^{-5}$ M). Moreover, measurements with C_nTABs at 800 Hz have shown that the elasticity increases even up to concentrations of about 10^{-3} M before the maximum is reached.[9,29]

In Figure 7b the $|\epsilon|(c)$ curves of β-$C_{12}G_2$ and $C_{10}E_4$ at $\nu =$ 0.1 Hz are plotted together with the corresponding high-frequency limits of the elasticity, which were calculated according to eq 6a. Note that again the amplitude $|\epsilon|$ has been determined to be able to compare the results with those obtained for C_{13}DMPO in Figure 7a. The corresponding elasticities ϵ and

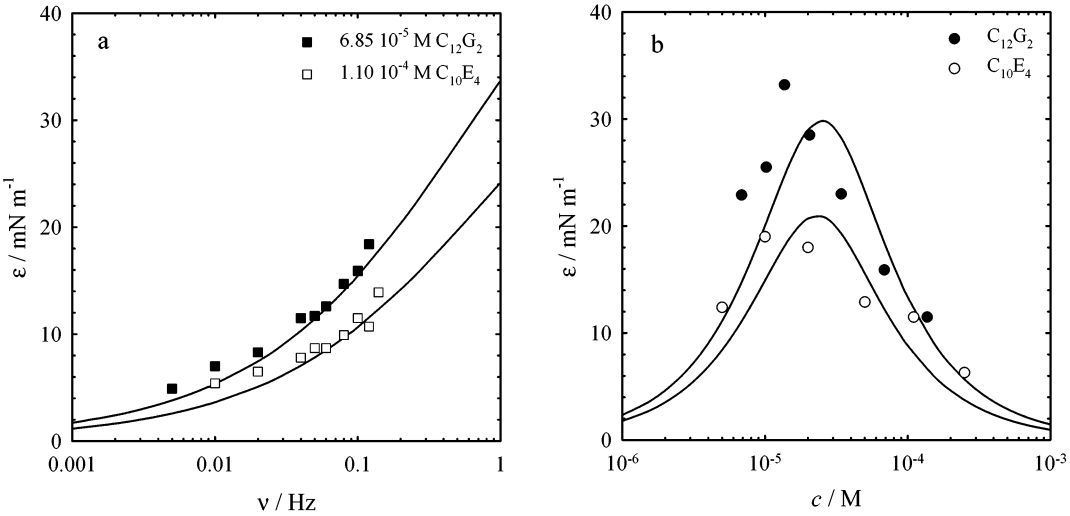

Figure 8. Dilational surface elasticities ϵ (a) of solutions containing 6.85×10^{-5} M β-$C_{12}G_2$ and 1.1×10^{-4} M $C_{10}E_4$, respectively, as a function of the frequency ν and (b) of β-$C_{12}G_2$ and $C_{10}E_4$ at 0.1 Hz as a function of the concentration c. Data are taken from Figures 4 and 6.

the phase angles ϕ are listed in Table A1 (see Appendix). Comparing the data of the three different surfactants one clearly sees that the concentration dependence at $\nu = 0.1$ Hz is qualitatively the same. Moreover, for C_{13}DMPO and β-$C_{12}G_2$ the results agree nearly quantitatively, whereas the corresponding $|\epsilon|$ values of $C_{10}E_4$ are lower in accordance with the results shown in Figure 5. It goes without saying that experiments at higher frequencies are needed for β-$C_{12}G_2$ and $C_{10}E_4$ to complete the picture. Work with respect to this point is under way. Coming back to Figure 7b, one sees that the $|\epsilon|$ values of β-$C_{12}G_2$ are larger than those of $C_{10}E_4$ over the whole concentration range investigated. This is in perfect agreement with the observation that thin liquid foam films stabilized by β-$C_{12}G_2$ are much more stable than the corresponding $C_{10}E_4$ films. At first sight, the theoretical ϵ_0 values describe the same general trend, namely, lower elasticities of the $C_{10}E_4$ monolayers compared to the respective β-$C_{12}G_2$ monolayer. However, it is not the elasticity at a constant surfactant concentration that we are interested in, but at a constant surface potential. Obviously, the correlation between elasticity and foam film stability is much more complex and will therefore be discussed separately in the following section.

Last but not least, it has to be pointed out that the discrepancy between experimental and calculated data seen in Figure 6 is mainly due to the inaccurate theoretical description of the high-frequency limit ϵ_0. Possible reasons for the difficulties in determining exact ϵ_0 values were discussed in connection with Table 2.

3.4. Foam Film Stability from a Surface Rheology Point of View. Discussing the correlation between foam film stability and surface rheology, we need to recall the problems we are faced with. In Figure 1 it was seen that at $q_0 = 1.17$ mC m^{-2} the β-$C_{12}G_2$ film is much more stable than the corresponding $C_{10}E_4$ film. Moreover, for $C_{10}E_4$ a decrease of the surface charge from $q_0 = 1.17$ mC m^{-2} to $q_0 = 0.95$ mC m^{-2} is accompanied by an increasing film stability. As was discussed in the Introduction, neither of these observations can be explained in terms of surface forces. The question to be answered is whether these experimental observations can be explained by taking into account surface rheology. Those dilational surface elasticities ϵ that are of importance with respect to this question are shown in Figure 8.

We will first address the difference in the stabilities at equal surface forces (see Figure 1a). We measured the $\epsilon(\nu)$ curves of the same surfactant solutions with which the thin liquid films were stabilized. As can be seen in Figure 8a, the surface elasticity of β-$C_{12}G_2$ is larger than that of $C_{10}E_4$ over the whole frequency range investigated. Anticipating that the calculated $\epsilon(\nu)$ curves describe correctly both the low- and the high-frequency ranges, we can even argue that for this particular concentration the elasticity of β-$C_{12}G_2$ is higher than that of $C_{10}E_4$ at any frequency. This is a very important result because it is not clear yet which is the relevant frequency with respect to the stability of free-standing foam films. Supposing that film rupture is caused by thermally induced thickness and concentration fluctuations (refs 1, 10, 12, 31, and references therein), it is the high-frequency range that should be of relevance. In this respect measurements with the excited capillary wave technique[9,29] in a frequency range from 200 to 800 Hz as well as surface light scattering[32−34] at frequencies from 5 to 400 kHz would be of interest.

Let us now discuss the second observation that we cannot explain by means of surface forces, i.e., that a decrease of the surface charge density is accompanied by an increase in the film stability (see $\Pi(h)$ curves of $C_{10}E_4$ in Figure 1a,b). To answer this question, the surface rheological parameters were measured as a function of the concentration. The surface elasticities obtained at $\nu = 0.1$ Hz are presented in Figure 8b. For the relevant concentrations, i.e. 1.1×10^{-4} M and 5.0×10^{-4} M $C_{10}E_4$, we can see that the surface elasticity of the latter is lower than that of the former. At first sight this result seems to be illogical. As was already discussed in section 3.3, however, the shape of the $\epsilon(c)$ curve depends on the interplay of the frequency of disturbance ν and the molecular exchange parameter ω_0. In our particular case it holds that $\omega_0 > \nu$, which, in turn, leads to a decrease of ϵ with increasing concentration. However, as has been discussed with respect to Figure 8a, the frequency of relevance for film rupture is supposed to be at much higher frequencies than those investigated in the present study. As an increase in ν shifts the maximum of the $\epsilon(c)$ curve to higher concentrations, a frequency will be reached at which $\epsilon(1.1 \times 10^{-4}\ \text{M}) < \epsilon(5.0 \times 10^{-4}\ \text{M})$. Based on $\epsilon(\nu)$ curves measured at concentrations above 10^{-4} M (alkyl dimethyl phosphine oxides in ref 19, $C_{10}E_8$ in ref 35, $C_{10}E_5$ in ref 17, C_nTABs in refs 9, 29) this frequency is expected to be between 200 and 800 Hz. Work to expand our data to higher frequencies is under way.[36]

To conclude, one can say that the observation of different film stabilities at equal surface forces demonstrated in Figure 1a can be explained by the surface elasticities ϵ of the corresponding monolayers: the higher stability of the β-$C_{12}G_2$ film is mirrored in the higher ϵ values. So far, a correlation between the surface elasticity and the corresponding $\Pi-h$ curves has only been discussed for the cationic alkyl trimethylammonium bromides (C_nTAB). For this particular homologous series a strong increase of ϵ is observed when the chain length is increased from $n = 12$ to $n = 14$.[9,29] A further increase of the chain length does not have any significant influence. Comparing these results with the fact that the respective films are only stable for $n > 12$,[1] one can conclude that foam film stability and surface elasticity are directly correlated. However, the surface rheology study of the C_nTAB series was restricted to two different frequencies and the respective foam film stabilities were investigated for only one particular concentration. Thus the study at hand is the first of its kind where both a broad concentration and frequency range were investigated. To complete our data, measurements at higher frequencies are planned. Note that it is only a complete set of $\epsilon-c$ and $\epsilon-\nu$ curves that will enable us to quantify the correlation between the surface elasticity and the pressure threshold for film rupture. Moreover, these curves are needed to clarify whether thermally induced thickness and concentration fluctuations affect the DLVO forces. A promising concept to describe the correlation between fluctuations and DLVO forces was published by Bergeron.[1,31] It is proposed that the energy needed to create these fluctuations could be a function of both the surface elasticity ϵ and the disjoining pressure Π. The lower the surface elasticity, the higher the fluctuations and the higher the probability to exceed the energy barrier, i.e., Π_{max}. Therefore, the surface elasticity and the pressure threshold for film rupture are expected to be correlated, first experimental evidence of which is provided by the results presented in the paper at hand.

4. Conclusions

In the paper at hand the dilational surface elasticities ϵ and the dilational surface viscosities η of the two nonionic surfactants *n*-dodecyl-β-D-maltoside (β-$C_{12}G_2$) and tetraethyleneglycol-monodecyl ether ($C_{10}E_4$) were measured as a function of the concentration and the frequency. The frequency range investigated was 0.005−0.2 Hz, and the solutions correspond to those investigated previously in a disjoining pressure study. The $\Pi(h)$ curves of this study revealed that the stability of the foam films cannot be explained solely by the magnitude of the surface forces: systems with equal surface forces can have completely different stabilities. It is discussed in the relevant literature that a stable film requires elastic surfaces to dampen external disturbances and thus to prevent the film from rupturing. In contrast to the interaction forces, which operate normal to the interface, the surface elasticity absorbs energy tangentially to the film surface. A first direct correlation between the pressure above which the film ruptures and the dilational elasticity of the film's surfaces is given here. The higher stability of the β-$C_{12}G_2$ film at $q_0 = 1.17$ mC m^{-2} compared to that of the respective $C_{10}E_4$ film is directly mirrored in the higher ϵ values of β-$C_{12}G_2$. However, what is still missing for these particular systems is a systematic analysis of the theoretical limiting elasticities ϵ_0 as a function of concentration based on optimum thermodynamic models including the recently introduced intrinsic compressibility of a covered surface layer. Moreover, measurements at higher frequencies are strongly needed. These measurements are expected to lead to the conclusion that the increasing stability with decreasing surface charge observed for $C_{10}E_4$ is due to an increase of the surface elasticity. It is only a complete set of $\epsilon(c)$ and $\epsilon(\nu)$ curves that will enable us to improve existing concepts and to quantify the correlation between the surface elasticity and the pressure threshold for film rupture.

In addition to the question about the correlation between surface rheology and film stability we are also faced with the problem that the surface rheology of the surfactant monolayers might not be the relevant parameter to describe the film stability. At least at film thicknesses where interaction forces come into play it is the elasticity of the whole film rather than that of the single surface that has to be considered. In other words, as soon as interaction forces play a role, the properties of the film cannot be derived from the properties of its single surfaces. To tackle this problem, Nagarajan et al. developed a tensiometer for measuring the rheological behavior of liquid films.[37−39] During the experiment a film is expanded very rapidly and its response is measured in terms of film tensions. The initial (maximum) film tension after the expansion is used to determine the film elasticity. It is claimed that the film expansion is so fast that there is no time for surfactant adsorption; that is, the experiment is believed to be carried out at the high-frequency limit. However, the high-frequency limit depends strongly on the surfactant concentration, so that even a fast expansion might not be fast enough to prevent surfactants from adsorbing to the surface. What is needed is an analogue to the oscillating bubble tensiometer, i.e., an oscillating film tensiometer.

Acknowledgment. C.S. is indebted to the FCI, the Ministerium für Wissenschaft und Forschung des Landes NRW, and the DFG for financial support. We also acknowledge very helpful discussions with V. B. Kovalchuk, Kiev.

Appendix

One of the experimental challenges is to determine the phase shift ϕ between the sinusoidal disturbance and the answer of

TABLE A1: Real Part ϵ and Amplitude $|\epsilon|$ of the Complex Modulus $\bar{\epsilon}$ (eq A1) for Six Different Concentrations of β-$C_{12}G_2$ and $C_{10}E_4$[a]

β-$C_{12}G_2$						
c/M	1.02×10^{-5}	1.37×10^{-5}	2.05×10^{-5}	3.42×10^{-5}	6.85×10^{-5}	1.37×10^{-4}
ϵ/mN m^{-1}	25.5	33.2	28.5	23	16	11.5
ϕ/deg	13 ± 2	19	23	30	34	36
$\lvert\epsilon\rvert$/mN m^{-1}	26.2 ± 0.4	35	31	26.6	19.3	14.2
$C_{10}E_4$						
c/M	5×10^{-6}	1×10^{-5}	2×10^{-5}	5×10^{-5}	1.1×10^{-4}	2.5×10^{-4}
ϵ/mN m^{-1}	12.4 ± 0.6	18.8 ± 0.2	18	13 ± 0.2	11.5	6.3
ϕ/deg	12 ± 2	16 ± 1	14	35 ± 2	26 ± 2	31
$\lvert\epsilon\rvert$/mN m^{-1}	12.7 ± 0.7	19.6 ± 0.2	18.6	15.8 ± 0.7	12.8 ± 0.2	7.3

[a] $|\epsilon|$ was calculated according to $|\epsilon| = \epsilon/\cos\phi$ with ϕ being the phase shift between sinusoidal disturbance and response. All values have been measured at a constant frequency of $\nu = 0.1$ Hz.

the monolayer. If this phase shift cannot be extracted from the experimental data, it is only the amplitude $|\epsilon|$ of the complex modulus $\bar{\epsilon}$ that can be determined experimentally. It holds

$$\bar{\epsilon} = |\epsilon| \exp(i\phi) = |\epsilon|\cos\phi + i|\epsilon|\sin\phi = \epsilon + i\omega\eta \tag{A1}$$

with

$$\epsilon = |\epsilon|\cos\phi \tag{A2}$$

and

$$\eta = \frac{|\epsilon|}{\omega}\sin\phi \tag{A3}$$

The frequency and concentration dependence of the amplitude $|\epsilon|$ is given by[18]

$$|\epsilon|(\nu,c) = \epsilon_0 \frac{1}{\sqrt{1 + 2\xi + 2\xi^2}} \tag{A4}$$

To illustrate the correlation between ϵ and $|\epsilon|$, some selected values are listed in Table A1 as a function of the concentration. The experiments have all been performed at 0.1 Hz. The data are presented in Figures 6 and 7, respectively.

References and Notes

(1) Bergeron, V. *Langmuir* **1997**, *13*, 3474.

(2) Karraker, K. A. Thesis, Berkeley, 1999.

(3) Stubenrauch, C.; Schlarmann, J.; Strey, R. *Phys. Chem. Chem. Phys.* **2002**, *4*, 4504; *Phys. Chem. Chem. Phys*. **2003**, *5*, 2736

(4) Schlarmann, J.; Stubenrauch, C. *Tenside Surf. Det.* **2003**, *40*, 190.

(5) Schlarmann, J.; Stubenrauch, C.; Strey, R. *Phys. Chem. Chem. Phys.* **2003**, *5*, 184.

(6) Exerowa, D.; Kruglyakov, P. M. In *Foam and Foam Films—Theory, Experiment, Application*; Möbius, D., Miller, R., Eds.; Elsevier: Amsterdam, 1998.

(7) In films stabilized by aqueous solutions of nonionic surfactants electrostatic repulsive forces are acting. It is well-accepted that the charges are due to a specific adsorption of OH^- ions at the water/air interface. However, an adsorption model is still missing. A detailed discussion on this issue can be found in ref 8.

(8) Stubenrauch, C.; Klitzing, R. v. *J. Phys.: Condens. Matter* **2003**, *15*, R1197.

(9) Monroy, F.; Giermanska-Khan, J.; Langevin, D. *Colloids Surf. A* **1998**, *143*, 251.

(10) Langevin, D. *Adv. Colloid Interface Sci.* **2000**, *88*, 209.

(11) Fruhner, H.; Wantke, K.-D.; Lunkenheimer, K. *Colloids Surf. A* **2000**, *162*, 193.

(12) Stubenrauch, C. *Tenside Surf. Det.* **2001**, *38* (6), 350.

(13) Stubenrauch, C.; Schlarmann, J.; Strey, R. *Phys. Chem. Chem. Phys.* **2003**, *5*, 2736.

(14) Loglio, G.; Pandolfini, P.; Miller, R.; Makievski, A. V.; Ravera, F.; Ferrari, M.; Liggieri, L. In *Novel Methods to Study Interfacial Layers*; Möbius, D., Miller, R., Eds.; Elsevier: Amsterdam, 2001.

(15) Gaydos, J. In *Drops and Bubbles in Interfacial Research*; Möbius, D., Miller, R., Eds.; Elsevier: Amsterdam, 1998.

(16) (a) Lucassen, J.; van den Tempel, M. *Chem. Eng. Sci.* **1972**, *27*, 1283. (b) Lucassen, J.; van den Tempel, M. *J. Colloid Interface Sci.* **1972**, *41*, 491.

(17) Jayalakshmi, Y.; Ozanne, L.; Langevin, D. *J. Colloid Interface Sci.* **1995**, *170*, 358.

(18) Wantke, K.-D.; Fruhner, H.; Fang, J.; Lunkenheimer, K. *J. Colloid Interface Sci.* **1998**, *208*, 34.

(19) Wantke, K.-D.; Fruhner, H. *J. Colloid Interface Sci.* **2001**, *237*, 185.

(20) Kovalchuk, V. I.; Krägel, J.; Makievski, A. V.; Loglio, G.; Ravera, F.; Liggieri, L.; Miller, R. *J. Colloid Interface Sci.* **2002**, *252*, 433.

(21) Fainerman, V. B.; Miller, R.; Kovalchuk, V. I. *Langmuir* **2002**, *18*, 7748.

(22) Fainerman, V. B.; Miller, R.; Kovalchuk, V. I. *J. Phys. Chem. B* **2003**, *107*, 6119.

(23) Kovalchuk, V. I.; Loglio, G.; Fainerman, V. B.; Miller, R. *J. Colloid Interface Sci.* **2004**, *270*, 475.

(24) Lunkenheimer, K.; Haage, K.; Hirte, R. *Langmuir* **1999**, *15*, 1052.

(25) The diffusion coefficients can be considered only as rough estimates as long as the theoretical model with which they are calculated is not improved. For example, a detailed study of the adsorption kinetics of $C_{10}E_4$ (Lee, Y.-C.; Liu, H.-S.; Lin, S. Y. *Colloids Surf. A* **2003**, *212*, 123) led to a diffusion coefficient of 7.2×10^{-10} m^2 s^{-1} instead of 2.5×10^{-10} m^2 s^{-1}.

(26) Lucassen, J.; Giles, D. *J. Chem. Soc., Faraday Trans. 1* **1975**, *71*, 217.

(27) Lucassen, J. In *Anionic Surfactants: Physical Chemistry of Surfactant Action*; Lucassen-Reynders, E. H., Ed.; Marcel Dekker: New York, 1981.

(28) Lucassen-Reynders, E. H.; Cagna, A.; Lucassen, J. *Colloids Surf. A* **2001**, *186*, 63.

(29) Stenvot, C.; Langevin, D. *Langmuir* **1988**, *4*, 1179.

(30) The theoretical $|\epsilon|(c)$ curves for C_{13}DMPO are not shown. This is due to the fact that the calculated ϵ values are up to 6 times larger than the experimental ones. Possible reasons for these large discrepancies are given in the text.

(31) Bergeron, V. *J. Phys.: Condens. Matter* **1999**, *11*, R215.

(32) Langevin, D., Ed. In *Light Scattering by Liquid Surfaces and Complementary Techniques*; Marcel Dekker: New York, 1992.

(33) Earnshaw, J. C. *Adv. Colloid Interface Sci.* **1996**, *1*, 68.

(34) Sharpe, D.; Eastoe, J. *Langmuir* **1996**, *12*, 2303.

(35) Liggieri, L.; Attolini, V.; Ferrari, M.; Ravera, F. *J. Colloid Interface Sci.* **2002**, *255*, 225.

(36) For frequencies up to 100 Hz a modified version of the oscillating bubble technique can be used with which the changes in surface tension are monitored by a sensitive pressure transducer[18,35] instead of monitoring the drop shape by a video camera. For higher frequencies the excited capillary wave technique[9,29] can be used.

(37) Nagarajan, R.; Wasan, D. T. *J. Colloid Interface Sci.* **1993**, *159*, 164.

(38) Nagarajan, R.; Koczo, K.; Erdos, E.; Wasan, D. T. *AIChE J.* **1995**, *41*, 915.

(39) Kim, Y-.H.; Koczo, K.; Wasan, D. T. *J. Colloid Interface Sci.* **1997**, *187*, 29.